

## Monosubstituted Conjugated Acetylide-Thiourea Derivatives as Active Layer in Conductive Film

Amirah Nabilah Rashid<sup>a</sup>, Rafizah Rahamathullah<sup>a,b</sup> and Wan M. Khairul<sup>a\*</sup>

<sup>a</sup>*School of Fundamental Science, Universiti Malaysia Terengganu, 21030 Kuala Terengganu, Terengganu, Malaysia.*

<sup>b</sup>*Faculty of Engineering Technology, Universiti Malaysia Perlis, 02100 Padang Besar, Perlis, Malaysia.*

\*Corresponding author: [wmkhairul@umt.edu.my](mailto:wmkhairul@umt.edu.my)

### Abstract

Works on conjugated molecules comprising of acetylide and thiourea moieties mimicking the function as macro devices are surprisingly not widely explored even though this system is proven to be an excellent candidate in various molecular electronic applications. They individually offers electronic delocalization in extended  $\pi$ -orbital system that contributes in electrical conductivity. Due to these concerns, a novel acetylide-thiourea derivative namely *N*-(3,5-dimethoxy benzoyl)-*N'*-(4-(phenylethynyl)phenyl) thiourea (DBPT) was successfully designed, synthesized and characterized via CHNS, IR, UV-Vis, <sup>1</sup>H and <sup>13</sup>C NMR, TGA and Cyclic Voltammetry (CV). The active layer of DBPT was deposited on ITO substrate via electrochemical deposition method (ECD) and then its conductivity was evaluated by using Four-Point Probe. The electrical conductivity test showed that the film formed has an ability to conduct electricity up to 0.2008 Scm<sup>-1</sup> under maximum light intensity of 150 Wm<sup>-2</sup>. Therefore, it is undoubtedly that the proposed single molecule of acetylide-thiourea has displayed a good performance to act as conductive film as well as has provided a great interest for a new field of research topic to be explored in diverse application.

**Keywords:** acetylide, thiourea, conductive film, molecular wire

### 1. INTRODUCTION

Conductive films are usually used as electrodes for numerous electro optical devices such as organic light emitting diodes (OLEDs), liquid crystal displays (LCDs), solar cells and gas sensors [1-4]. Most of these conductive films are constructed of indium

tin oxide (ITO) as substrate since it exhibits favourable features like good conductivity, stable, excellent optical transparency and low electrical resistivity [2-6]. Designing new organic materials with electron conjugation property to act as an active layer in conductive films has gained much interest since they required low production cost, light weight and easy fabrication process [7].

For these reasons, a conductive film was fabricated from a conjugated organic molecule containing an acetylide-thiourea moiety. In this study, the presence of conjugation in molecular framework of the mixed moieties featuring thiourea and acetylide gives enormous advantages especially in designing single molecular wire system. The delocalized  $\pi$ -electrons over the conjugated chain make relatively good conductors of electricity [8, 9]. This electrical conductivity behaviour also aroused from the resonance process occurred among the lone pair of electrons from N, O and S atoms in thiourea. In contrast to thiourea, the acetylide derivative has extended rigid  $\pi$ -system arising from double and triple bonds but it is still resulted in distribution of electric charge all over the molecule.

Hence, apart from low cost of production, simple and easy synthetic work-up, acetylide-thiourea derivative (DBPT) as illustrated in Figure 1 is utterly has the potential to act as single conjugated molecular wire and eventually, it can operate as dopant system in conductive film.

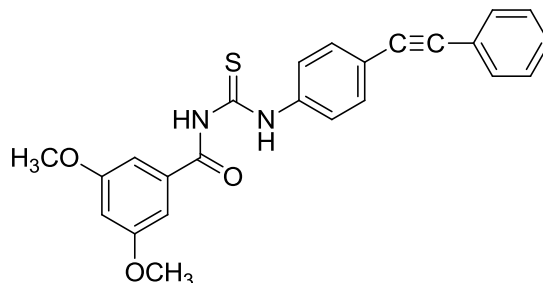


**Figure 1.** Molecular structure of *N*-(3,5-dimethoxy benzoyl)-*N'*-(4-(phenylethynyl)phenyl) thiourea (DBPT)

## 2. EXPERIMENTAL

### 2.1. Materials

All chemicals and solvents used in this study were commercially available from Merck, Sigma Aldrich, BiosynTech and HmbG® Chemicals and were used as received without further purification. The synthetic works involved in this study were carried out under an ambient condition.

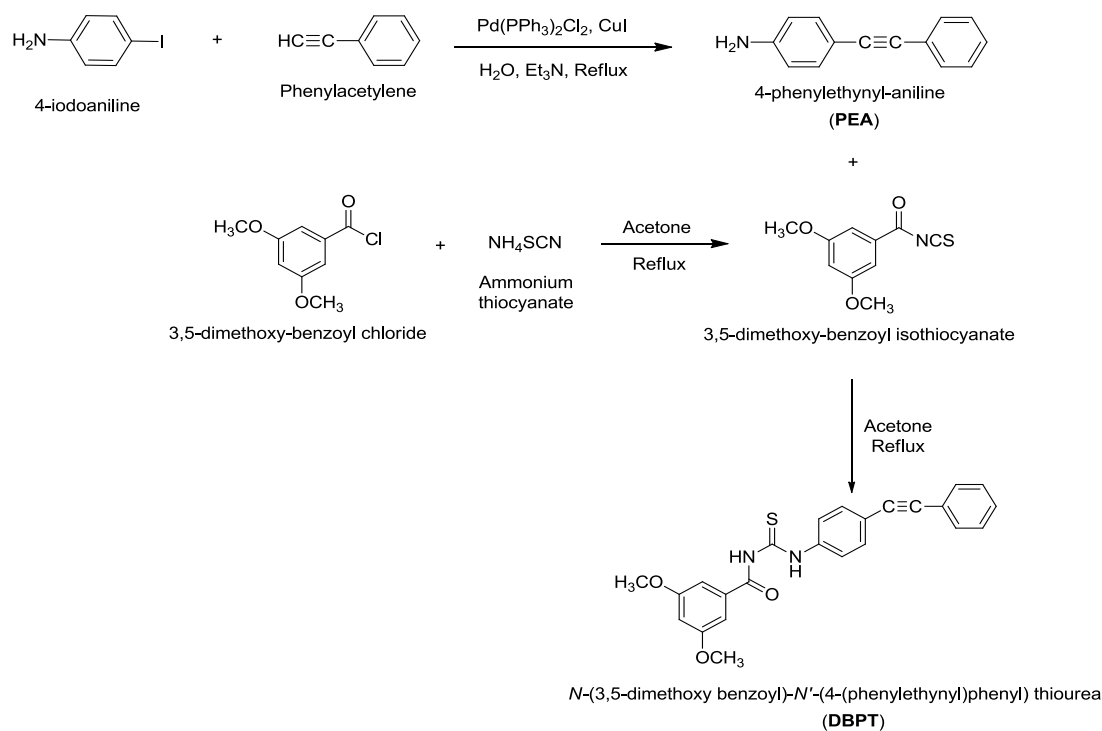
### 2.2. Instrumentation

Infrared (IR) spectra of the synthesized compounds were recorded on Perkin Elmer 100 Fourier Transform Infrared Spectroscopy by using the conventional potassium bromide

(KBr) pellet method in the range of 4000-400  $\text{cm}^{-1}$ . Meanwhile for UV-Vis spectroscopy, the UV spectra were recorded using Spectrophotometer Shimadzu UV-1601PC in 1  $\text{cm}^3$  cuvette in acetonitrile solution with concentration of  $1 \times 10^{-5}$  M. In addition,  $^1\text{H}$  (400.11 MHz) and  $^{13}\text{C}$  (100.61 MHz) NMR spectroscopy analyses were conducted by using Bruker Avance III 400 spectrometer in deuterated chloroform ( $\text{CDCl}_3$ ). For thermal investigation, TGA analysis was carried out using Perkin-Elmer TGA Analyzer from 30  $^\circ\text{C}$  to 800  $^\circ\text{C}$  with 10  $^\circ\text{C}/\text{min}$  heating rate under nitrogen surrounding. CHNS Analyzer Flash EA 1112 series was used to obtain the mass fractions of C, H, N and S atoms of the synthesized compounds while the melting point of the targeted molecule was analyzed by using Stuart Scientific Melting Point Apparatus SMP3. Next, Cyclic Voltammetry (CV) analysis was conducted to find out the possibilities of redox potential by using three-electrode cell system of glassy carbon working electrode, a platinum counter electrode and a reference electrode with scan rate of 0.05 V/s. Afterwards, the electrical conductivity of the films was measured under different light intensities by using Four-Point Probes equipment.

### 2.3. Synthetic Work

There were two main steps involved in this study. Firstly, the precursor of acetylide derivative namely 4-phenylethynyl-aniline (PEA) was synthesized, followed by the synthesis of acetylide-thiourea molecule, *N*-(3,5-dimethoxy benzoyl)-*N'*-(4-(phenylethynyl)phenyl) thiourea (DBPT). Scheme 1 illustrates the overall pathway for the synthetic works involved.



**Scheme 1.** Synthetic pathway for the preparation of DBPT

### 2.3.1. Synthesis of 4-phenylethynyl-aniline (PEA)

The synthetic work to obtain the precursor of PEA followed the reported method in literature [10-12] with some modification was carried out in this protocol. The reaction involved 4-iodoaniline (3.0 g, 13.7 mmol) and phenylacetylene (2.1 mL, 20.55 mmol) in the mole ratio (1:1.5) via Sonogashira cross-coupling reaction, catalyzed by 5% mmol of each Pd(PPh<sub>3</sub>)<sub>2</sub>Cl<sub>2</sub> and CuI. The mixture was then put at reflux temperature and constant stirring for *ca.* 24 hours in triethylamine (40 mL) and distilled water (40 mL) forming two distinct layers of solution. When adjudged completion by thin layer chromatography (TLC) using (hexane:dichloromethane; 3:2) as eluent, the reaction mixture cooled to room temperature and washed with dichloromethane. Then, purification via column chromatography using hexane and dichloromethane was conducted to afford brown solid of PEA (1.57 g, 59 %). C<sub>14</sub>H<sub>11</sub>N (theoretical): C, 87.01; H, 5.74; N, 7.25, (experimental): C, 87.81; H, 5.70; N, 7.07. IR (KBr):  $\nu$ (N-H) 3475 cm<sup>-1</sup> and 3379 cm<sup>-1</sup>,  $\nu$ (C-H) 3037 cm<sup>-1</sup>,  $\nu$ (C≡C) 2211 cm<sup>-1</sup>. <sup>1</sup>H NMR (CDCl<sub>3</sub>, 400.11 MHz):  $\delta$ <sub>H</sub> 3.70 (s, 2H, NH<sub>2</sub>); 6.53 (pseudo-d, <sup>3</sup>J<sub>HH</sub>= 8Hz, 2H, C<sub>6</sub>H<sub>4</sub>); 7.16-7.27 (m, 5H, C<sub>6</sub>H<sub>5</sub>); 7.40 (pseudo-d, <sup>3</sup>J<sub>HH</sub>= 8Hz, 2H, C<sub>6</sub>H<sub>4</sub>). <sup>13</sup>C NMR (CDCl<sub>3</sub>, 100.61 MHz):  $\delta$ <sub>C</sub> 87.34, 90.11 (C≡C); 112.68, 113.40, 127.40, 128.41, 131.60, 132.85 (6 x Ar-C); 146.63 (C-N). Melting point: 126.9-128.3 °C.

### 2.3.2. Synthesis of N-(3,5-dimethoxy benzoyl)-N'-(4-(phenylethynyl)phenyl) thiourea (DBPT)

An equivalent mole ratio of 3,5-dimethoxy-benzoyl chloride (0.42 g, 2.09 mmol) and ammonium thiocyanate (0.16 g, 2.09 mmol) were dissolved separately in *ca.* 30 mL acetone. The chloride was added drop wise to the solution of ammonium thiocyanate to give pale pink solution and the mixture was then put at reflux and stirred for *ca.* 5 hours. Once adjudged completion by TLC using eluent system (hexane:ethyl acetate; 3:2), the reaction mixture was filtered to remove salt and the filtrate was cooled to room temperature. Next, the solution of PEA (0.40 g, 2.09 mmol) in *ca.* 30 mL acetone was added drop wise into the filtered solution. The reaction was then left refluxed and stirred for another *ca.* 4 hours, giving a yellowish-brown solution. Few ice cubes were added and the precipitate collected underwent recrystallization from methanol to yield yellow crystalline solids of the targeted DBPT (0.74 g, 85 %). C<sub>24</sub>H<sub>20</sub>N<sub>2</sub>O<sub>3</sub>S (theoretical): C, 69.21; H, 4.84; N, 6.73; S, 7.70, experimental: C, 68.74; H, 4.98; N, 6.88; S, 7.76. IR (KBr):  $\nu$ (N-H) 3404 cm<sup>-1</sup>,  $\nu$ (C-H) 3030 cm<sup>-1</sup>,  $\nu$ (C=O) 1671 cm<sup>-1</sup>,  $\nu$ (C-O) 1335 cm<sup>-1</sup>,  $\nu$ (C=S) 736 cm<sup>-1</sup>,  $\nu$ (C≡C) 2216 cm<sup>-1</sup>. <sup>1</sup>H NMR (CDCl<sub>3</sub>, 400.11 MHz):  $\delta$ <sub>H</sub> 3.79 (s, 6H, 2 x OCH<sub>3</sub>); 6.64 (s, 1H, C<sub>6</sub>H<sub>3</sub>); 6.91 (pseudo-d, <sup>3</sup>J<sub>HH</sub>= 2Hz, 2H, C<sub>6</sub>H<sub>4</sub>); 7.28, 7.29 (s, 2 x 1H, C<sub>6</sub>H<sub>3</sub>); 7.46-7.52 (m, 5H, C<sub>6</sub>H<sub>5</sub>); 7.72 (pseudo-d, <sup>3</sup>J<sub>HH</sub>= 8Hz, 2H, C<sub>6</sub>H<sub>4</sub>); 8.97 (s, 1H, N-H (C=O)); 12.64 (s, 1H, N-H (C=S)). <sup>13</sup>C NMR (CDCl<sub>3</sub>, 100.61 MHz):  $\delta$ <sub>C</sub> 55.77 (2 x CH<sub>3</sub>); 88.84, 90.21 (C≡C); 105.34-137.40 (Ar-C); 161.39 (C-O); 166.93 (C=O); 177.69 (C=S). Melting point: 176.3-178.1 °C.

### 2.4. Fabrication and Electrical Conductivity Test of DBPT film on ITO Substrate

The fabrication of DBPT with 1x10<sup>-3</sup> M concentration in 50 mL acetonitrile solution on the ITO substrate was conducted via electrochemical deposition (ECD) method using Electrochemical Impedance Spectroscopy (EIS) PGSTAT 302 instrument. Figure

2 illustrates the architectural design of DBPT/ITO.

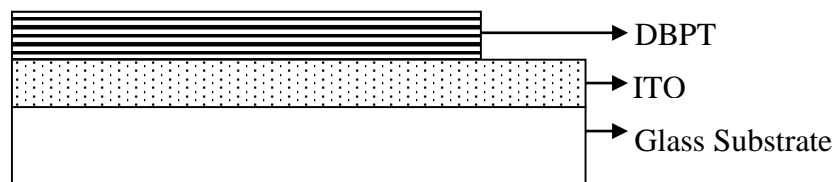


**Figure 2.** Design of the conductive organic film

Next, Four-Point Probe system consisting of Jandel Universal Probe and Jandel RM3 Test Unit were used to measure the sheet resistivity of the prepared films. In this study, the performance of the films prepared in conducting electricity was examined in the dark and under different light intensities (50, 100 and 150 Wm<sup>-2</sup>). In turn, from the current and voltage data attained from the Four-Point Probe analysis, the sheet resistivity,  $R_S$ , value can be determined using the (Equation 1) [13-16]:

Average resistance of the film:

$$R_S = 4.53 \times (V/I) \quad \text{(Equation 1)}$$

Where,  $R_S$  is the electrical resistance of the film; 4.53 is the geometric factor;  $V$  is the output voltage measured across the inner probes with the voltmeter and  $I$  is the constant current applied through the two outer probes. The electrical conductivity,  $\sigma$ , is the inverse of the electrical resistivity,  $R_S$ , where it can be calculated by using (Equation 2):

$$\sigma = 1/ R_S \quad \text{(Equation 2)}$$

Where,  $\sigma$  = electrical conductivity and  $R_S$  = electrical resistance of the film.

### 3. RESULTS AND DISCUSSION

#### 3.1. Infrared (IR) Spectroscopic Analysis

From the analysis conducted, there were six major distinct bands of interest observed in the targeted acetylide-thiourea compound (DBPT) namely  $\nu(\text{N-H})$  3404 and 3287 cm<sup>-1</sup>,  $\nu(\text{C-H})$  3030 cm<sup>-1</sup>,  $\nu(\text{C=O})$  1671 cm<sup>-1</sup>,  $\nu(\text{C-O})$  1335 cm<sup>-1</sup>,  $\nu(\text{C=S})$  736 cm<sup>-1</sup> and  $\nu(\text{C}\equiv\text{C})$  2216 cm<sup>-1</sup>. Two bands were recorded at high frequency region of 3404 and 3287 cm<sup>-1</sup> as the acetylide-thiourea ligand showed two different pairs of asymmetric  $\nu(\text{N-H})$  stretching vibrations. These values were almost similar as reported by [17] as they stated one of the  $\nu(\text{N-H})$  values can be found above 3200 cm<sup>-1</sup> and the other one can be seen at above 3000 cm<sup>-1</sup> due to the presence of intramolecular hydrogen bonding N-H...O=C. The existence of major bands C=O and C=S indicating that DBPT was indeed a thiourea derivative where the bands fall in the similar range as reported by

other studies [18, 19]. Strong IR absorption of  $\nu(\text{C}=\text{O})$  at  $1671\text{ cm}^{-1}$  was found at lower frequency for typical carbonyl double bonds due to its intramolecular hydrogen bonding with N-H moiety [17, 20, 21]. Moreover, the band corresponding to the asymmetric and symmetric  $\nu(\text{C}=\text{S})$  stretching vibration of thiourea appeared at  $736\text{ cm}^{-1}$  was in good agreement with previous studies [17, 22, 23]. On the other hand,  $\nu(\text{C}\equiv\text{C})$  band of the acetylide-thiourea moiety which recorded at  $2216\text{ cm}^{-1}$  was strongly supported by the literature [12, 24, 25, 26].

### 3.2. Ultraviolet-visible (UV-vis) spectroscopy

UV absorption data reveals the important and expected electronic transitions and contribution of chromophores namely C=C (aromatic), C=O and C=S moieties around  $\lambda_{\text{max}} = 250\text{ nm}$  and  $350\text{ nm}$ , proving the synthesized compound of DBPT in this study is indeed a thiourea compound. The bands observed in the region of  $250 - 315\text{ nm}$  were assigned to the  $\pi \rightarrow \pi^*$  transition of the aromatic moiety as the values are in good agreement as reported by [12, 27]. The  $\pi \rightarrow \pi^*$  and  $n \rightarrow \pi^*$  transitions of C=S usually located at around  $\lambda_{\text{max}} 275\text{ nm}$  and therefore it can be concluded that there was overlapping between C=O band which also resulted in a broad absorption band observed in the region [28]. On the other hand, a bathochromic shift was observed for DBPT arises from the extended  $\pi$ -conjugation which usually found in ethynyl derivatives [25]. The absorption band of C=C was not observed because its transitions are rather at high energy and their positions are sensitive to the presence of any substituent. However, typically the absorption of alkynes usually can be observed at around  $170\text{ nm}$  [28].

### 3.3. $^1\text{H}$ and $^{13}\text{C}$ Nuclear Magnetic Resonance (NMR)

For  $^1\text{H}$  NMR of DBPT, the obvious moieties that can be observed were the methoxy (-OCH<sub>3</sub>), primary amines (-NH) and aromatic protons. The methoxy protons were located at  $\delta_{\text{H}} 3.79\text{ ppm}$  which was at the higher chemical shift than usual due to the deshielding effect arising from the oxygen atom that is a more electronegative atom located near its position where the value was close with previous report [29]. Primary amine (N-H) was detected at two different position of  $\delta_{\text{H}} 8.97\text{ ppm}$  and  $\delta_{\text{H}} 12.64\text{ ppm}$  due to the different electronegative atoms placed next to it. Since sulphur atom is more electronegative, the N-H proton attached next to it can be observed at the most deshielded area and the other resonance belongs to N-H proton that attached next to C=O. Besides, the difference in chemical shift value of these two signals was because of the electron-withdrawing effect as well as the intramolecular hydrogen bond occurred in the molecule [30-32]. On the other hand, aromatic protons were observed around the range of  $\delta_{\text{H}} 6.64 - 7.72\text{ ppm}$  corresponded to three phenyl rings presence in the compound.

Meanwhile for  $^{13}\text{C}$  NMR of DBPT, the resonances recorded were O-CH<sub>3</sub>, C=C, Ar-C, C-O, C=O and C=S. The methoxy resonance can be clearly detected at  $\delta_{\text{C}} 55.77\text{ ppm}$  which is slightly higher in chemical shift value compared to the typical value due to the present of more electronegative oxygen atom next to it [33]. Next, carbon resonances for alkyne were observed at  $\delta_{\text{C}} 88.84$  and  $90.21\text{ ppm}$  which were in good agreement as reported by [34]. The resonances of aromatic ring carbons were located in the range of

$\delta_c$  105.34 – 137.40 ppm which close to the value reported by previous study [32, 35] while C-O resonance on the other hand was assigned at  $\delta_c$  161.39 ppm. Last but not least, the most deshielded  $^{13}\text{C}$  NMR signals correspond to C=O and C=S resonances appeared at  $\delta_c$  166.93 ppm and 177.69 ppm respectively due to the electronegativity factor [36]. The thiocarbonyl carbon has the highest value whereas the carbonyl group is the second most deshielded because of the intra-molecular hydrogen bond associated to the oxygen atom of the carbonyl group [17, 35].

#### **3.4. Thermogravimetric Analysis (TGA)**

From the thermogram obtained, there was an early degradation process occurred during the thermal analysis at below 100 °C. This usually happened because of the drying stage and removal of the trapped solvent and water [37]. DBPT has gone through two dominant degradation phases where the first one took place at around 180 °C ( $T_{\text{onset}}$ ) with maximum degradation of 235 °C ( $T_{\text{max}}$ ) and ended at around 330 °C ( $T_{\text{offset}}$ ). On the other hand, the second decay phase began to degrade at 350 °C ( $T_{\text{onset}}$ ) and ended at 475 °C ( $T_{\text{offset}}$ ) with maximum degradation of 400 °C ( $T_{\text{max}}$ ). Based on the data obtained, high onset and offset temperature probably occurred due to the heavy molecular weight which required higher temperature to degrade the sample. Besides, a thiourea derivative which has conjugated system and overlapping orbitals between C=S and C=O also resulted in higher value of onset temperature [38].

However, around 400 °C, all of the organic part of the samples would have decomposed and so all the samples were heat-treated at that temperature [39] and in this study, DBPT underwent the highest temperature of degradation around 500 °C. This property has showed that DBPT has high thermal stability thus give an advantage for it to be applied as conductive film.

#### **3.5. Cyclic Voltammetry (CV) Analysis**

The electrochemical analysis was conducted with DBPT ( $1 \times 10^{-3}$  M) in acetonitrile and addition of 0.5 M sulphuric acid as supporting electrolyte on glassy carbon electrode at 0.05 V/s scan rate. The cyclic voltammogram revealed an irreversible redox process with the presence of both oxidation and reduction peaks respectively as shown in Figure 3:

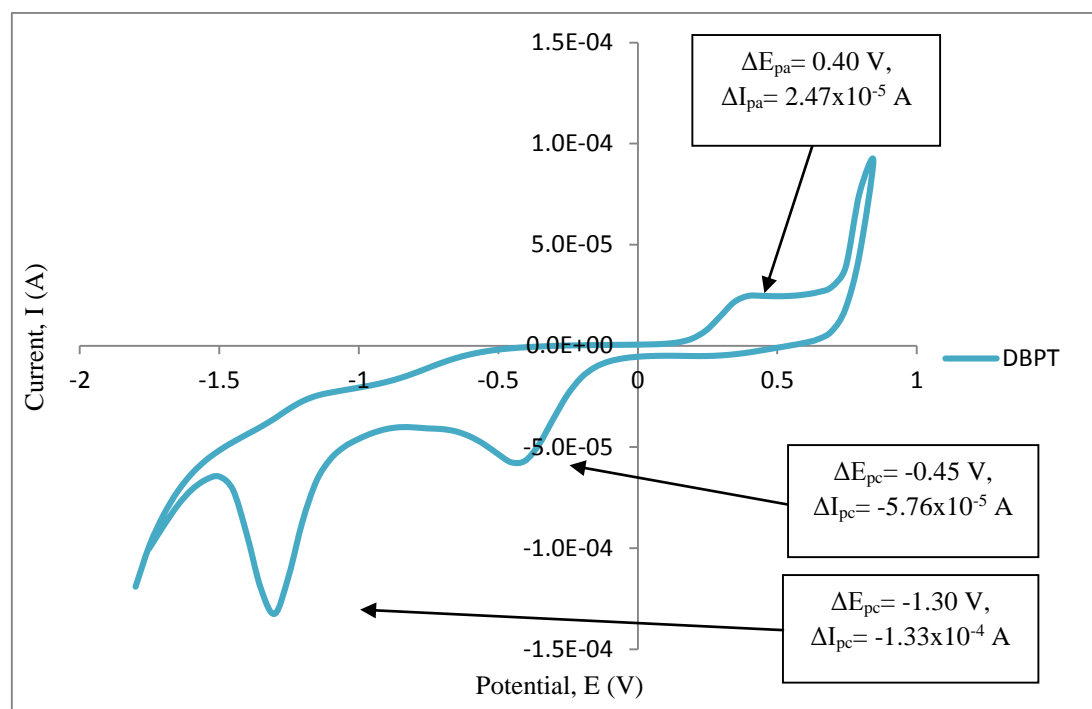


**Figure 3.** Voltammogram of DBPT in acetonitrile with addition of 0.5 M sulphuric acid

The oxidation peak took place at  $\Delta E_{pa} = 0.40$  V with  $\Delta I_{pa} = 2.47 \times 10^{-5}$  A, while the reduction peak occurred at  $\Delta E_{pc} = -0.45$  V with  $\Delta I_{pc} = -5.76 \times 10^{-5}$  A and  $\Delta E_{pc} = -1.30$  V with  $\Delta I_{pc} = -1.33 \times 10^{-4}$  A. There are several reports that formamidine disulfide (FDS) ions are formed as a result from the oxidation process of thiourea and comparing to the work done by [40] that process occurred at a potential of  $\sim 0.5$  V which is almost similar with the result obtained from this study. It is also suggested that the cathodic peak occurred at the negative potential value attributed to the reduction of FDS [40]. From the cyclic voltammetry analysis, a better result of the redox process occurred in the range of  $-1.8$  V to  $+0.8$  V. Therefore, it can be concluded that the synthesized compounds exhibit redox potential which give a good sign for the potential of film fabrication to be applied as conductive film.

### 3.6. Electrical Conductivity Analysis

The electrical conductivity study in film form coated on ITO substrate were tested by using Four-Point Probe under dark and various light intensity condition ( $\text{Wm}^{-2}$ ). Figure 4 shows the graphical result of the electrical conductivity of DBPT.

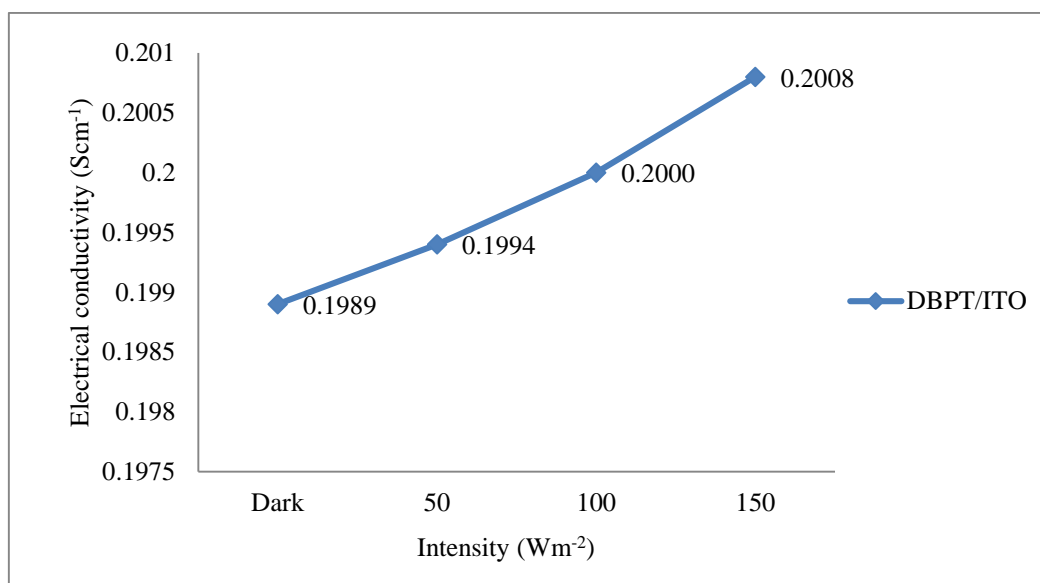


**Figure 4.** The electrical conductivity of DBPT/ITO

From the test carried out, the conductivity increases as the light intensity increases. Besides that, DBPT also has the ability to conduct electricity even under the dark condition. This is probably because of the extended  $\pi$ -conjugation system arising from  $C\equiv C$ ,  $C=O$ ,  $C=S$  and  $C=C$  (Ar) moieties that produces electricity even without the presence of light. This is because the free movement of  $\pi$ -electrons along the conjugated chain gives good conductors of electricity [8, 9]. Thus, under maximum light intensity of  $150 \text{ Wm}^{-2}$ , DBPT/ITO showed the highest reading of  $0.2008 \text{ Scm}^{-1}$  and eventually, it is proven that DBPT has the potential to be applied as an active layer in conducting material.

## CONCLUSION

A new member of monosubstituted acetylide-thiourea derivative namely *N*-(3,5-dimethoxy benzoyl)-*N'*-(4-(phenylethynyl)phenyl) thiourea (DBPT) was successfully synthesized, characterized and evaluated for its electrical conductivity behaviour to be applied as active layer in conductive film. The electrical study revealed the layer of DBPT/ITO film has the ability to conduct electricity even with the absence of light and under various light intensities. The highest conductivity data recorded was  $0.2008 \text{ Scm}^{-1}$  under light intensity of  $150 \text{ Wm}^{-2}$ . Therefore, the proposed acetylide-thiourea system has proven to be an interesting candidate to be explored in depth due to its potential to be applied as single conjugated molecular wire in various microelectronic applications.

## ACKNOWLEDGEMENTS

The authors would like to address special acknowledgement to the Ministry of Higher Education Malaysia (MOHE) for research grant (FRGS 59253), MyBrain Fund for

postgraduate student's scholarship, School of Fundamental Science and Institute of Marine Biotechnology (IMB) Universiti Malaysia Terengganu for the facilities provided.

## REFERENCES

- [1] Xu, W., Xu, Q., Huang, Q., Tan, R., Shen, W., and Song, W., 2016, "Fabrication of Flexible Transparent Conductive Films with Silver Nanowire by Vacuum Filtration and PET Mold Transfer," *Journal of Materials Science & Technology*, 32, pp. 158-161.
- [2] Wan, G., Wang, S., Zhang, X., Huang, M., Zhang, Y., Duan, W., and Yi, L., 2015, "Transparent conductive Nb-doped TiO<sub>2</sub> films deposited by RF magnetron co-sputtering," *Applied Surface Science*, 357, pp. 622-625.
- [3] Liu, C.-C., Liu, T.-Y., Wang, K.-S., Tsou, H.-M., Wang, S.-H., and Chen, J.-S., "The polar solvent effect of transparent conductive films composed of graphene/PEDOT:PSS nanohybrids," *Surface & Coatings Technology*. In press.
- [4] Zhao, W., Nugay, I. I., Yalcin, B., and Cakmak, M., "Flexible, stretchable, transparent and electrically conductive polymer films via a hybrid electrospinning and solution casting process: In-plane anisotropic conductivity for electro-optical applications," *Displays*. In press.
- [5] Chen, Y., Lan, W., Wang, J., Zhu, R., Yang, Z., Ding, D., Tang, G., Wang, K., Su, Q., and Xie, E., 2016, "Highly flexible, transparent, conductive and antibacterial films made of spin-coated silver nanowires and a protective ZnO layer," *Physica E.*, 76, pp. 88-94.
- [6] Yu, J.-S., Jung, G. H., Jo, J., Kim, J. S., Kim, J. W., Kwak, S.-W., Lee, J.-L., Kim, I., and Kim, D., 2013, "Transparent conductive film with printable embedded patterns for organic solar cells," *Solar Energy Materials & Solar Cells*, 109, pp. 142-147.
- [7] Vegiraju, S., Hsieh, C.-M., Huang, D.-Y., Chen, Y.-C., Priyanka, P., Ni, J.-S., Esya, F. A., Kim, C., Yau, S. L., Chen, C.-P., Liu, C.-L., and Chen, M.-C., 2016, "Synthesis and characterization of solution-processable diketopyrrolopyrrole (DPP) and tetrathienothiophene (TTA)-based small molecules for organic thin film transistors and organic photovoltaic cells," *Dyes and Pigments*, 133, pp. 280-291.
- [8] Li, Y., and Yang, M., 2002, "Transition metal acetylide catalysts for polymerization of alkynes 5. Homogeneous copolymerization of polar with non-polar alkynes," *Journal of Molecular Catalysis A: Chemical*, 184, pp. 161-165.
- [9] Tress, W., 2014, "Organic Solar Cells: Theory, Experiment, and Device Simulation," Switzerland: Springer International Publishing.
- [10] Rosseto, R., Torres, J. C., and Nero, J. D., 2003, "Modeling of Alkynes: Synthesis and Theoretical Properties," *Materials Research*, 6(3), pp. 341-346.
- [11] Greenberg, S., and Stephan, D. W., 2010, "Hydroamination as a route to

- nitrogen-containing oligomers,” *Polymer Chemistry*, 1, pp. 1332-1338.
- [12] Daud, A. I., Khairul, W. M., Zuki, H. M., and Kubulat, K., 2015, “Aerobic synthetic approach and characterisation of some acetylide-thiourea derivatives for the detection of carbon monoxide (CO) gas,” *Journal of Molecular Structure*, 1093, pp. 172-178.
- [13] Gou, J., Tang, Y., Liang, F., Zhao, Z., Firsich, D., and Fielding, J., 2010, “Carbon nanofiber paper for lightning strike protection of composite materials,” *Composites: Part B.*, 41, pp. 192-198.
- [14] Henry, J., Mohanraj, K., and Sivakumar, G. 2016, “Electrical and optical properties of CZTS thin films prepared by SILAR method,” *Journal of Asian Ceramic Societies*, 4, pp. 81-84.
- [15] Ogwu, A. A., Darma, T. H., and Bouquerel, E., 2007, “Electrical resistivity of copper oxide thin films prepared by reactive magnetron sputtering,” *Journal of Achievements in Materials and Manufacturing Engineering*, 24, pp. 172-177.
- [16] Mwathe, P., Musembi, R., Munji, M., Odari, V., Munguti, L., Ntilakigwa, A., Nguu, J., and Muthoka, B., 2014, “Effect of Surface Passivation on Electrical Properties of Pd-F:SnO<sub>2</sub> Thin Films Prepared by Spray Pyrolysis Technique,” *Coatings*, 4, pp. 747-755.
- [17] Karipcin, F., Atis, M., Sariboga, B., Celik, H., and Tas, M., 2013, “Structural, spectral, optical and antimicrobial properties of synthesized 1-benzoyl-3-furan-2-ylmethyl-thiourea,” *Journal of Molecular Structure*, 1048, pp. 69-77.
- [18] Jusoh, R. H., Khairul W. M., Yusof, M. S. M., Kadir, M. A., and Yamin, B. M., 2011, “Structural and spectroscopic studies of novel methylbenzoylthiourea derivatives,” *The Malaysian Journal of Analytical Sciences*, 15(1), pp. 70-80.
- [19] Rahamathulla, R., Khairul, W. M., Salleh, H., Adli, H. K., Isa, M. I. N., and Tay, M. G., 2013, “Synthesis, characterization and electrochemical analysis of V-shaped disubstituted thiourea-chlorophyll thin film as active layer in organic solar cells,” *International Journal of Electrochemical Science*, 8, pp. 3333-3348.
- [20] Saeed, A., Erben, M. F., and Bolte, M., 2013, “Synthesis, structural and vibrational properties of 1-(adamantane-1-carbonyl)-3-halophenyl thioureas,” *Spectrochimica Acta Part A: Molecular and Biomolecular Spectroscopy*, 102, pp. 408-413.
- [21] Saeed, A., Khurshid, A., Bolte, M., Fantoni, A. C., and Erben, M. F., 2015, “Intra- and intermolecular hydrogen bonding and conformation in 1-acyl thioureas: An experimental and theoretical approach on 1-(2-chlorobenzoyl)thiourea,” *Spectrochimica Acta Part A: Molecular and Biomolecular Spectroscopy*, 143, pp. 59-66.
- [22] Gil, D. M., Lestard, M. E. D., Estévez-Hernández, O., Duque, J., and Reguera, E., 2015, “Quantum chemical studies on molecular structure, spectroscopic (IR, Raman, UV-Vis), NBO and Homo–Lumo analysis of 1-benzyl-3-(2-furoyl)thiourea,” *Spectrochimica Acta Part A: Molecular and Biomolecular Spectroscopy*, 145, pp. 553-562.
- [23] Kanagasabapathy, K., and Rajasekaran, R., 2013, “Growth aspects, spectral, thermal and hardness studies of rare earth cerium(III)nitrate doped zinc(tris) thiourea sulphate single crystals,” *Optik*, 124, pp. 4240-4245.

- [24] Lee, Y. O., Pradhan, T., No, K., and Kim, J. S., 2012, "*N,N*-Dimethylaniline and 1-(trifluoromethyl)benzene-functionalized tetrakis(ethynyl)pyrenes: synthesis, photophysical, electrochemical and computational studies," *Tetrahedron*, 68, pp. 1704-1711.
- [25] Gama, P. E., Corrêa, R. J., and Garden, S. J., 2015, "Synthesis, characterization and photophysical study of ethynyl pyrene derivatives as promising materials for organic optoelectronics," *Journal of Luminescence*, 161, pp. 37-46.
- [26] Khairul, W. M., Daud, A. I., Zuki, H. M., and Kubulat, K., 2015, "Theoretical and Spectroscopic Studies of *N*-([4-aminophenyl]ethynyltoluene)-*N'*-(1-naphthanoyl thiourea (ATT) as Carbon Monoxide Gas Chemosensor," *Applied Mechanics and Materials*, 719-720, pp. 59-62.
- [27] Saad, F. A., 2014, "Synthesis, spectral, electrochemical and X-ray single crystal studies on Ni(II) and Co(II) complexes derived from 1-benzoyl-3-(4-methylpyridin-2-yl) thiourea," *Spectrochimica Acta Part A: Molecular and Biomolecular Spectroscopy*, 128, pp. 386-392.
- [28] Pavia, D. L., Lampman, G. M., Kriz, G. S., and Vyvyan, J. A., 2013, "Introduction to Spectroscopy," Fifth Edition, Cengage Learning.
- [29] Giesen, J. M., Claborn, K. A., Goldberg, K. I., Kaminsky, W., and West, D. X., 2002, "Structural, thermal and spectral studies of *N*-2-pyridyl-, *N*-2-picoly- and *N*-2-(4,6-lutidyl)-*N'*-(3-methoxyphenyl)thioureas," *Journal of Molecular Structure*, 613, pp. 223-233.
- [30] Khairul, W. M., Roslan, N. A., Rahamathullah, R., and Salleh, H., 2014, "Picoline Thiourea Derivative Doped with *Lawsonia inermis* Dye as Active Layer in Potential Organic Solar Cell," *Malaysian Journal of Microscopy*, 10, pp. 62-70.
- [31] Kelman, D. R., Claborn, K. A., Kaminsky, W., Goldberg, K. I., and West, D. X., 2002, "Structural, spectral and thermal studies of *N*-2-(pyridyl)- and *N*-2-(picoly)-*N'*-(3-chlorophenyl)thioureas," *Journal of Molecular Structure*, 642, pp. 119-127.
- [32] Tahir, S., Badshah, A., Hussain, R. A., Tahir, M. N., Tabassum, S., Patujo, J. A., and Rauf, M. K., 2015, "DNA-binding studies and biological activities of new nitrosubstituted acyl thioureas," *Journal of Molecular Structure*, 1099, pp. 215-225.
- [33] Selvakumaran, N., Bhuvanesh, N. S. P., Endo, A., and Karvembu, R., 2014, "Synthesis, structure, DNA and protein binding studies, and cytotoxic activity of nickel(II) complexes containing 3,3-dialkyl/aryl-1-(2,4-dichlorobenzoyl)thiourea ligands," *Polyhedron*, 75, pp. 95-109.
- [34] Xu, Z., Mei, Q., Hua, Q., Tian, R., Weng, J., Shi, Y., and Huang, W., 2015, "Synthesis, characterization, energy transfer and photophysical properties of ethynyl bridge linked porphyrin-naphthalimide pentamer and its metal complexes," *Journal of Molecular Structure*, 1094, pp. 1-8.
- [35] Atiş, M., Karıpcin, F., Sariboğa, B., Taş, M., and Çelik, H., 2012, "Structural, antimicrobial and computational characterization of 1-benzoyl-3-(5-chloro-2-hydroxyphenyl)thiourea," *Spectrochimica Acta Part A: Molecular and Biomolecular Spectroscopy*, 98, pp. 290-301.

- [36] Arslan, N. B., Kazak, C., and Aydin, F., 2012, "*N*-(4-Nitrobenzoyl)-*N'*-(1,5-dimethyl-3-oxo-2-phenyl-1*H*-3(2*H*)-pyrazolyl)-thiourea hydrate: Synthesis, spectroscopic characterization, X-ray structure and DFT studies," *Spectrochimica Acta Part A: Molecular and Biomolecular Spectroscopy*, 89, pp. 30-38.
- [37] Alshehri, S. M., Al-Fawaz, A., and Ahamad, T., 2013, "Thermal kinetic parameters and evolved gas analysis (TG-FTIR-MS) for thiourea-formaldehyde based polymer metal complexes," *Journal of Analytical and Applied Pyrolysis*, 101, pp. 215-221.
- [38] Adli, H. K., Khairul, W. M., and Salleh, H., 2012, "Synthesis, Characterization and Electrochemical Properties of Single Layer Thin Film of *N*-Octyloxyphenyl-*N'*-(4-Chlorobenzoyl)Thiourea-Chlorophyll As Potential Organic Photovoltaic Cells," *International Journal of Electrochemical Science*, 7, pp. 499-515.
- [39] Martis, P., Fonseca, A., Mekhalif, Z., and Delhalle, J., 2010, "Optimization of cuprous oxide nanocrystals deposition on multiwalled carbon nanotubes," *J. Nanopart. Res.*, 12, pp. 439-448.
- [40] Shevtsova, O. N., Bek, R. Y., Zelinskii, A. G., and Vais A. A., 2006, "Anodic Behavior of Gold in Acid Thiourea Solutions: A Cyclic Voltammetry and Quartz Microgravimetry Study," *Russian Journal of Electrochemistry*, 42(3), pp. 279-285.

